UCRL-94073
PREPRINT

SYSTEM AND SITE NOISE IN THE REGIONAL SEISMIC TEST NETWORK

P. W. Rodgers
S. R. Taylor
K. K. Nakanishi

Submitted to: Bulletin Seismological Society of America

February, 1986

Lawrence Livermore National Laboratory

Abstract

The Regional Seismic Test Network (RSTN) consists of five broadband, three-component, telemetered seismic stations sited in North America in 100 m boreholes. Examination of both the system noise and the seismic site noise at these stations leads to the following conclusions:

(i) The vertical short-period (SP) band data are not degraded by quantizing noise, even at very low levels (< 0.1 nm^2/Hz @ 1 Hz). This is also the case for mid-period (MP) band signals.

(ii) Small MP band signals which are grossly quantized (1.28 mV/count) due to the presence of a simultaneous large amplitude signal retain a sufficient number of counts for resolution of small events. The approximate threshold is an Lg arrival from an event $m_b(Lg) = 2.5$ at 20^o epicentral distance.

(iii) Aliasing in the SP band causes significant distortion above 16 Hz.

(iv) The seasonal average vertical earth noise at 1 Hz at the RSTN stations range from $0.07^{nm}/Hz$ (RSNT) to $1.8^{nm}/Hz$ (RSNY) and the average rolloff is -2 $nm/\sqrt{Hz/Hz}$ (proportional to f^{-2}). Above 1 Hz RSCP is the noisiest and RSNT the quietest station.

(v) At RSNT during quiet times, some of the observed noise may be due to the vertical component S-750 seismometer.

It is our conclusion that there is no significant system contamination of regional seismic data recorded by the RSTN and that it records these data with good fidelity.

INTRODUCTION

The Department of Energy's Regional Seismic Test Network (RSTN) consists of five broadband, three component, satellite telemetered seismic stations sited in 100 m boreholes in the U.S. and Canada, in Tennessee(RSCP), Northwest Territories(RSNT), New York(RSNY), Ontario(RSON) and South Dakota(RSSD), (Fig. 1). The purpose of the RSTN is both to determine the seismic capabilities of such a regional network and to serve as an engineering testbed and provide operational experience for a similar system which would possibly be deployed in-country for monitoring compliance with a comprehensive nuclear test ban treaty.

Two different types of three component seismometers, the Teledyne-Geotech K-36000-04 and S-750, are deployed in each borehole. Both types of instruments are feedback stabilized seismometers. The S-750 is used solely as the short period sensor in the normal configuration of the network. Analog filters separate the output from each component into three bands: short- period (SP), 1-10 Hz; mid-period 0.05-1 Hz; (MP), and long-period (LP), 0.015-.055 Hz; The velocity sensitivity curves for the three bands are shown in Fig. 2. A detailed description of the RSTN system is given by Stokes (1982), Breding (1983), and Taylor (1983).

To some extent, the ability of each RSTN station to faithfully record small seismic events is determined both by the noise and distortions within the system itself and by the ambient earth noise at each site. It is the purpose of this study to address these various sources of noise and distortion and to evaluate them in terms of the quality and limitations of the RSTN data.

There are two categories of noise occurring within the RSTN which are treated in this paper:

1. Noise generated by the system itself. This system noise includes both noise which is generated by a system component such as the seismometer and noise due to distortions within the system caused by the sampling and quantization of the data.

2. Seismic noise at the RSTN site. This is earth noise due to both natural and cultural sources which is recorded at the particular RSTN site. Only the vertical component of noise is treated.

QUANTIZING NOISE IN THE SP BAND

In this section we investigate the effect of quantizing noise on SP band data.

A block diagram of the SP band channel is shown in Fig. 3. The analog voltage output of the S-750, which is proportional to acceleration, is low pass filtered (approximately integrated) to change it to velocity and then band pass filtered to produce the SP band response shown in Fig. 2. The amplitude of this signal is adjusted by means of the four step gain ranger and passed to the analog-to-digital-converter (ADC).

Quantizing noise is introduced into the system by the process of discretizing the analog voltage which is performed by the 16 bit ADC. Two of these bits are used for the gain ranging multiplier and one for sign leaving the remaining thirteen bits for resolution of the signal (Breding, 1983). This corresponds to a dynamic range of 120 db (78 db of resolution plus 42 db of gain ranging). The quantizing noise has a white spectrum with a mean squared value (MS) given by (c.f. Stearns, 1975):

$$MS = \frac{(\Delta V)^2}{12} \quad , \quad \text{volts}^2 \tag{1}$$

where ΔV is the least significant bit (LSB) in volts.

For low level signals, the gain ranger can be expected to be at its highest gain, X128. Therefore the LSB voltage, ΔV, is given by:

$$\Delta V = \frac{10.48 \text{ volts}}{128 \times 2^{13} \text{ counts}} = 9.99 \ \mu\text{volts/count} \tag{2}$$

The MS value of the quantizing noise given in Eq.(1) results in a power spectral density (PSD), P_{QQ}, given by (Appendix A):

$$P_{QQ} = \frac{(\Delta V)^2}{12} \ \Delta T \ , \ \text{volts}^2/\text{Hz} \tag{3}$$

3 component seismometer	Low Pass filter and Analog SP band filter	Gain Ranging amplifier	Analog to digital converter
S-750	SP	X8 X32 X128	ADC

Figure 3

where ΔT is the sampling period which is .025 sec in the short period band the RSTN. Equation (3) is the PSD of the quantizing noise at the output of the SP band filter shown in Fig. 3. In order to compare the quantizing noise with low level ground motions, it is useful to express it in terms of ground displacement PSD. It is also shown in Appendix A that the equivalent quantizing noise PSD in terms of ground displacement is given by:

$$\text{Quantizing noise PSD} = \frac{1}{\omega^2} \left|SP^{-1}\right|^2 \frac{(WV)^2}{12} \Delta T \qquad (4)$$

$$\left(\frac{nm^2}{Hz}\right) = (sec^2) \cdot \left(\frac{nm/sec}{volt}\right)^2 \cdot (volts)^2 \cdot \left(\frac{1}{Hz}\right)$$

where SP^{-1} is the inverse of the SP band response function. This theoretical quantizing noise PSD is plotted in Fig. 4.

As an additional check, the PSD of quantizing noise was also computed numerically from a synthetic noise seismogram (noisegram). A zero mean white Gaussian random voltage signal sampled at 40 sample/sec was generated. The peak amplitude of this signal rate was reduced to approximately ± 10 μvolts and the signal quantized using a 10 μV LSB. The result is a signal randomly switching between zero and ± 10 μV. The PSD of this signal was computed and corrected back to displacement PSD. The resulting displacement PSD, also shown in Fig. 4, agrees well with the theoretical PSD.

To determine if low level SP band signals in the RSTN are contaminated by this quantizing noise, a model of low level earth noise was simulated by passing a zero mean, 40 sample/sec, Gaussian random signal through both 2 pole and 3 pole low pass filters to obtain f^{-2} and f^{-3} rolloffs above 1 Hz. It will be shown in the section on site ground noise that these rolloffs bracket those measured for actual low level seismic noise. The signals were then quantized and their spectra corrected back to earth displacement

PSD as done previously. Further, the levels of the spectra were adjusted to 0.1 nm^2/Hz at 1 Hz which corresponds to the lowest site noise measured in this study. These two low earth noise models are plotted in Fig. 5 together with the quantizing noise. The f^{-2} model (which most closely models typical earth noise) is more than an order of magnitude above the quantizing noise for all frequencies. The f^{-3} model which is the worst case intersects the quantizing noise at approximately 16 Hz. Because the steepest rolloff we have observed for low level seismic noise at RSTN stations is $f^{-2.4}$, we conclude that the quantizing noise does not contaminate the RSTN SP band data.

QUANTIZING NOISE IN THE MP BAND

The quantizing noise for the MP band was computed by the method described previously for the SP band. The level in this band is higher than in the SP band because of the larger sampling interval [see eq (3)]. Figure 6 shows the level of the quantizing noise for these bands for minimum gain (G=1) and maximum gain (G=128). A plot of noise at RSNT (the lowest noise station) during a quiet time is superimposed for comparison. As can be seen, the quantizing noise for this case is several orders of magnitude below the ground noise for the MP band.

Because the microseismic peak at approximately 0.18 Hz occurs in the MP band, it is likely that the gain ranger is at a gain less than 128. In the worst case the gain ranger gain is 1 resulting in the quantizing noise curve labeled MP, (G=1) in Fig. 6. The intersection of this curve with the RSNT low noise curve implies that large amplitude MP band data will not be contaminated by quantizing noise out to beyond 0.7 Hz, which is close to the upper band edge. There may be some contamination of 1 Hz MP band data for the worst case situation.

GAIN RANGING DISTORTION IN THE MP BAND

As alluded to in the previous section, data in the MP band may be grossly quantized due to large amplitude signals (> 1.3106 volts) which drive the gain ranger to its lowest gain (X1). This results in quantization steps of 128 X 9.99 μV = 1.28 mV. This could occur for long periods of time during the arrival of a large amplitude long period surface wave from a distant earthquake. Gross quantization of MP band data could occur, for example, if a 1 sec. period Lg phase arrived during (i.e. on top of) a large excursion due to a long period Rayleigh wave. During time intervals the Rayleigh wave amplitude exceeds 1.306 volts, the gain ranger will be driven to its lowest gain, G=1. Therefore the accompanying Lg phase will be quantized in steps of 1.28 mV/count. The question is whether this will cause significant distortion of the Lg waveform. One way to address this question is the following. Consider an Lg arrival of magnitude m_b(Lg) = 2.5 from an event at 20^0 epicentral distance. This is certainly at the lower limit of detectability at that distance. Using the m_b(Lg) formula of Nuttli and Mitchell (1983) we find that for this small magnitude the vertical ground velocity is approximately 1160 nm/sec, peak to peak. Combining this with the MP band velocity sensitivity and the volts/count for G=1, we find the number of counts associated with this arrival:

$$\text{counts (peak-peak)} = \frac{5.3 \times 10^{-5} \frac{\text{volts}}{\text{nm/sec}}}{1.28 \times 10^{-3} \frac{\text{volts}}{\text{count}}} \times 1160 \text{ nm/sec} \sim 47 \text{ counts}$$

This is a sufficient number of peak to peak counts to resolve the threshold arrival; therefore we conclude that, in practice, the MP band distortion due to gain ranging is not a significant problem.

We have not addressed the effect which very large signals may have on the fidelity of the data. This has been partially treated by Taylor (1984) in his study of the Goodnow, NY earthquake as recorded at RSNY.

ALIASING IN THE SP BAND

In this section we perform a numerical experiment to study the effect of aliasing on the SP band data. As described in the previous section, synthetic noisegrams were generated with rolloffs of f^{-2} and f^{-3}; however the sampling rate used was 200 s/s resulting in a Nyquist frequency of 100 Hz. These 200 sample/sec synthetic noisegrams were passed through the SP band response, and thus represent the analog voltage signals out of the SP band filter. New signals were then generated by taking every fifth data point and quantizing the resulting 40 s/s data. This signal was then analogous to the gain-ranged and sampled signals in the RSTN.

For the f^{-2} model, Fig. 7 compares the PSD's of the 40 sample/sec aliased signal with the unaliased 200 sample/sec signal. The units are volts^2/Hz. Aliasing is clearly evident above 16 Hz. Figure 8 compares the PSD's of the 200 s/s and 40 s/s signals for the f^{-3} model. Aliasing is again evident, although less severe. The results are summarized in Fig. 9 which shows the percent of aliasing versus frequency for both the f^{-2} and f^{-3} models. The conclusion is that SP band data is contaminated by aliasing above 16 hz, at which frequency it may be as large as 8% depending on the rolloff of the signal. For close events, there may be significant high frequency energy resulting in a greater degree of aliasing.

HIGH-FREQUENCY SEISMIC NOISE AT THE RSTN STATIONS

Seismic noise originates from a number of different sources including cultural, microseismic, wind, etc. In a previous study, we reviewed characteristics of seismic noise in the band 0.01 - 5 Hz in the vicinity of the RSTN stations (Taylor, 1981, Taylor and Qualheim, 1982). In this section, we discuss noise spectra computed from noise samples at the RSTN stations in the frequency band between 0.1 - 20 Hz and compare the results with high frequency observations from other stations. Our emphasis will pertain to high frequency noise observations between about 0.5 to 15 Hz.

Five vertical-component noise samples were selected from the RSTN that were typically of 450 - 500s length (Table 1). To examine seasonal variability, three samples were selected in the winter and two in the summer. The noise power spectral density (PSD) was computed by dividing each sample into ten 50 second Hamming windows after prewhitening the data. Each window was fast-Fourier-transformed, the spectral values were averaged over all windows, and an autocorrelation function was computed from the average spectrum. Twenty seconds of the sample autocorrelation function were then used to obtain the PSD, giving 20 degrees of freedom in the spectral estimate.

The instrument-corrected power spectra are shown in Figs. 10-14 for the noise samples at each station. Examination of the spectra show that the variability of noise spectra is greater between stations of the RSTN than as a function of time at a given station. The stations show maximum differences of 10 - 20 dB with slightly greater differences observed at higher frequencies. At a given station, the spectra show maximum seasonal and diurnal variations of approximately 6 - 10 dB. The seasonal variations at the RSTN stations also show systematic differences. In general, the winter microseisms are shifted to lower frequencies (< 0.2 Hz) and are of higher

amplitude (~ 20 dB) than summer microseisms (which peak at approximately 0.2 - 0.25 Hz). These seasonal shifts in the microseismic peaks have been commonly observed in previous studies (see review in Taylor, 1981). At high frequencies, especially between 1 - 5 Hz (depending on the station), the summer noise levels are generally 3 - 6 dB higher than those in the winter.

The noise spectra also exhibit a number of well-defined high frequency noise spikes that often appear on all the noise samples. These spikes are particularly prominent at RSNT and have also been reported at other stations including Lajitas (Li et al., 1984), the SRO stations (Peterson, 1980), and at Albuquerque, NM (Farrell, 1979, Bache et al., 1985). The cause of these noise spikes is not well known and they exhibit numerous complications. For example, some noise spikes may be highly polarized as evidenced by their appearance on only one of three components (Rodgers and Broadwater, 1983; 1984). Additionally, some noise spikes may or may not be observed on both uphole and downhole recordings at the same site (Rodgers and Broadwater, 1983, 1984; Bache et al., 1985). Based on comparisons with surface and downhole sites at and nearby RSTN sites, Rodgers and Broadwater (1983; 1984) concluded that the source of many of the RSTN noise spikes may be related to unknown vibrations of the equipment at the site itself.

For each station, the spectra were averaged and are shown in Figure 15 along with the reported earth noise models at Queen Creek, Arizona (Brune and Oliver, 1959), from NORSAR (Bungum, 1983), and at Lajitas, Texas (Li et al., 1984). It should be noted that the RSTN spectra are from 100 m boreholes, while the other sites are nearsurface and would thus probably be slightly quieter at depth. The spectra are calculated to 8 Hz for RSCP (beyond which the response of the SP shaping filters drop off) and 20 Hz at the other four stations. However, the spectra show a flattening at approximately 16 Hz which is probably due to aliasing.

TABLE 1

SAMPLES USED FOR RSTN NOISE SPECTRA

DATE	START TIME(GMT)	LENGTH(sec)
1/5/83	02:00	450
1/8/83	11:20	500
1/24/83	12:48	500
6/9/83	13:01	400
7/24/83	18:07	450

The high frequency rolloffs determined by a linear regression between 1-10 Hz for the average spectra shown in Figure 15 are listed in Table 2. The average rolloff in $(nm/\sqrt{Hz})/Hz$ is -2.0 (f^{-2} or -40 dB/decade) and values range from -1.7 (-34 dB/decade) to -2.4 (-48 dB/decade). Stations characterized by higher noise values generally show flatter slopes. Additionally, as seen in Figs. 10-14, it appears that rolloffs in the summer season are generally less than those in the winter.

The average PSD values at 1 Hz are summarized for each station in Table 2. The average estimated peak to peak (P-P) noise values are also listed and were obtained using the technique outlined in Taylor (1981). At 1 Hz, the noise levels vary from 0.07 - 1.85 nm^2/Hz (-177 - 192 dB rel($1m^2/Hz$)) which convert to average P-P displacement noise levels of 0.5 - 2.7 nm. At 1 Hz, RSNY and RSCP appear to show the highest noise levels, followed by RSON, RSNT, and RSSD. At higher frequencies, RSCP appears to be the noisiest stations and RSNT the quietest.

SEISMOMETER NOISE IN THE SP BAND

Up to this point we have considered sources of noise and distortion in the RSTN system due to quantization, aliasing, gain ranging, and ground noise. The remaining noise source to be treated is that due to the seismometer. Because the SP band is commonly used for regional seismic signals, the SP band seismometer noise will be treated. The SP band seismometer is the Teledyne-Geotech S-750. As of July 1984, this seismometer is the sensor used in all three SP band components in the normal configuration of the RSTN.

The S-750 seismometer is unusual in that the relative motion between the 2 Kg mass and the frame is sensed by piezoelectric strain gages which measure the flexure strain in the suspension system. These signals are amplified to become the acceleration output, which is then fed back to a coil-magnet force

TABLE 2

SUMMARY OF NOISE SPECTRA AT RSTN STATIONS

STATION	avg. PSD(nm^2/Hz)	dB rel($1m^2$/Hz)	avg. P-P (nm)	rolloff(nm/$\sqrt{Hz}$/Hz)
RSCP	0.62	-182	1.6	-1.7 $\pm$ 0.11
RSNY	1.85	-177	2.7	-1.9 $\pm$ 0.04
RSON	0.20	-187	0.9	-1.8 $\pm$ 0.05
RSSD	0.07	-192	0.5	-2.2 $\pm$ 0.06
RSNT	0.09	-190	0.6	-2.4 $\pm$ 0.11

measurements taken at 1 Hz

balance transducer (Starkey, 1985). Extensive measurements and theoretical calculations of the self noise of the S-750 have been made by Durham (1984). Using the above data, the S-750 self noise power spectral density as it appears in the SP band was calculated. This is plotted in Fig. 16 in units of nm^2/Hz. For comparison purposes, the vertical earth noise at NORSAR (Bungum, 1983), Lajitas, Texas (Li et al., 1984) and RSNT during a very quiet period are also shown. As can be seen, the S-750 self noise is nearly the same as the RSNT quiet time noise. Because the RSNT noise was obtained from the S-750 SP band data and there is uncertainty regarding the exact level of seismometer self-noise, it is likely that some of the RSNT noise is coming from the S-750 and not the ground. As can be seen by comparing with the NORSAR and Lajitas noise curves, this is a problem only at low noise sites during very quiet times.

SUMMARY AND CONCLUSIONS

This paper has examined the RSTN system with the purpose of determining the effects of system and ground noise sources and distortions on data quality, principally in the SP band. The results are summarized as follows:

(i) Low level SP band data are not degraded by quantizing noise. The same is true for the MP and LP band data for the high gain case (G=128).

(ii) Small MP band signals which are grossly quantized (1.28 mV/count) due to the presence of a simultaneous large amplitude signal retain a sufficient number of counts for fidelity. The approximate threshold is an Lg arrival from an event having m_b(Lg) = 2.5 at 20^0 epicentral distance (~ 1160 nm/sec).

(iii) Aliasing causes significant distortion above 16 Hz in the SP band.

(iv) The seasonal average vertical earth noise at 1 Hz at the RSTN stations range from 0.07 nm^2/Hz (RSNT) to 1.8 nm^2/Hz (RSNY). The high frequency rolloff's vary from -1.7 to -2.4 $nm/\sqrt{Hz/Hz}$. Above 1 Hz RSCP is the noisiest and RSNT the quietest station.

(v) At RSNT during quiet times, some of the observed noise is probably due to the S-750 seismometer.

The conclusion which we reach from the above information is that there is no significant system contamination of regional data recorded by the Regional Seismic Test Networks and that these data are recorded with good fidelity.

ACKNOWLEDGMENTS

We have been assisted by useful conversations with many of our colleagues. Of particular help were discussions with H. B. Durham of Sandia Laboratories, Albuquerque and M. Denny and F. Followill of LLNL. Sandia National Laboratory also kindly supplied us with the seismic data for the site noise study. This work was performed under the auspices of the U.S. Department of Energy by the Lawrence Livermore National Laboratory under contract number W-7405-ENG-48.

Appendix A

Part I: Quantization Noise Power Spectral Density.

The rms value of quantizing noise is given in several texts as:

$$(\text{quant. noise})_{rms} = \frac{\Delta V}{\sqrt{12}} \qquad \text{(A-1)}$$

where ΔV is the volts/count. (c.f. Stearns, "Digital Signal Analysis, eq. (4-14). Therefore the mean squared value (MS) is

$$MS = \frac{(\Delta V)^2}{12}, \text{ volts}^2 \qquad \text{(A-2)}$$

The power spectral density which results in this MS value is uniformly distributed (white) from $-f_1$ to $+f_1$.

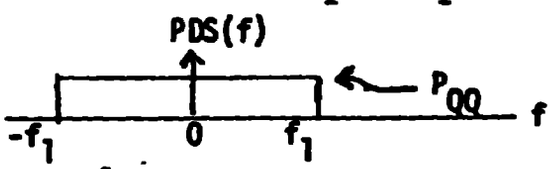

$$\text{So } MS = \int_{-f_1}^{f_1} P_{QQ}\, df = 2 \cdot P_{QQ} \cdot f_1 = \frac{(\Delta V)^2}{12} \qquad \text{(A-3)}$$

But from the sampling theorm, $f_1 = \frac{1}{2\Delta T}$

Solving for P_{VV} from (A-3) and eliminating f_1:

$$\boxed{P_{QQ} = \frac{(\Delta V)^2}{12} \cdot \Delta T, \text{ volts/Hz}^2} \qquad \text{(A-4)}$$

Part II: Obtaining quantization noise in equivalent nm^2/Hz.

The dynamics of the process of generating the output voltage from input ground velocity, the addition of quantizing noise voltage and the subsequent deconvolution back to estimated ground velocity can be represented by the block diagram below:

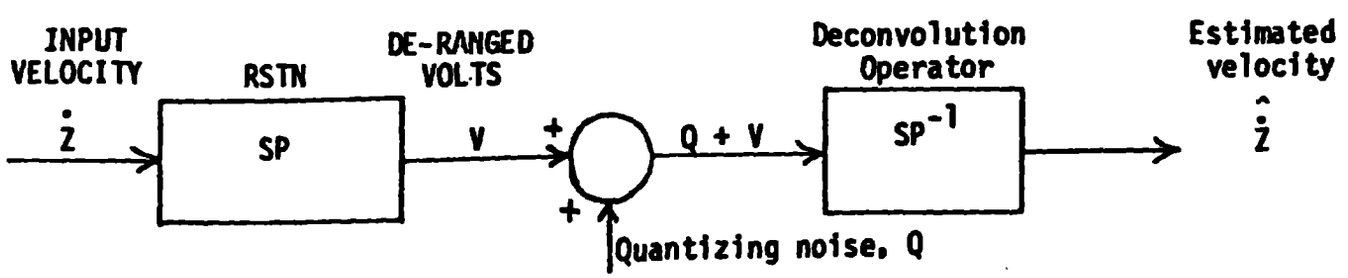

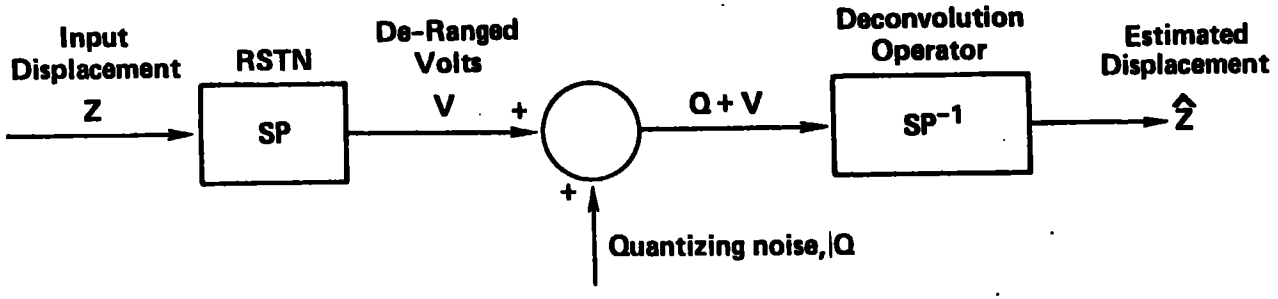
Input
Displacement
Z
RSTN
SP
De-Ranged
Volts
V
+
+
Quantizing noise, Q
Q + V
Deconvolution
Operator
SP^{-1}
Estimated
Displacement
$\hat{Z}$

In transformed quantities the steps can be written as

$$Z = SP^{-1}\,[SP \cdot Z + Q] = Z + SP^{-1}Q \qquad \text{(A-5)}$$

Since the quantizing noise Q is independent of Z, (A-5) can be written as follows in terms of power spectral densities of velocities:

$$P_{\dot{Z}\dot{Z}} = P_{\dot{Z}\dot{Z}} + \left|SP^{-1}\right|^2 \cdot P_{QQ} \qquad \text{(A-6)}$$

$$\frac{(nm/sec)^2}{Hz} = \frac{(nm/sec)^2}{Hz} + \frac{nm/sec}{volt}^2 \cdot \frac{volts^2}{Hz}$$

Usually displacement not velocity power densities are wanted. So rewriting (A-6) in displacement power by noting $\frac{\dot{Z}}{\omega} = Z$

$$P_{ZZ} = P_{ZZ} + \frac{1}{\omega^2}\left|SP^{-1}\right|^2 \cdot P_{QQ} \qquad \text{(A-7)}$$

$$\frac{nm^2}{Hz} = \frac{nm^2}{Hz} + sec^2 \cdot \frac{nm/sec^2}{volt} \cdot \frac{volts^2}{Hz}$$

The right hand term in (A-7) is the quantization noise in nm^2/Hz.

$$\text{Quantization noise in } nm^2/Hz = \frac{1}{\omega^2}\left|SP^{-1}\right|^2 \cdot \frac{(\Delta V)^2}{12} \cdot \Delta T \qquad \text{(A-8)}$$

This is the term which is plotted in Fig. 4 as the maximum gain quantizing noise. The minimum gain curve is larger by a factor of $(128)^2$. Notice that the curves are bent upward by the effect of the deconvolution operator on the white noise.

FIGURE CAPTIONS:

Fig. 1: Locations of Regional Seismic Test Network (RSTN) Stations. (Stokes, 1982)

Fig. 2: Velocity sensitivity response curves for the RSTN: Long period (LP), mid-period (MP), and short period (SP) bands.

Fig. 3: Short-period (SP) band block diagram.

Fig. 4: Comparison of theoretical and numerical SP band quantizing noise for high gain case, G=128.

Fig. 5: SP band quantizing noise (G=128) compared to f^{-2} and f^{-3} rolloff earth noise models.

Fig. 6: MP band quantizing noise (G=128, G=1) with RSNT quiet time earth noise.

Fig. 7: Test of aliasing in the SP band using f^{-2} rolloff earth noise model.

Fig. 8: Test of aliasing in the SP band using f^{-3} rolloff earth noise model.

Fig. 9: Percent aliasing in the SP band for f^{-2} and ω^{-3} rolloff earth noise models.

Fig. 10: Seismic noise at RSCP. Five time periods (see legend)

Fig. 11: Seismic noise at RSNT. Five time periods (see legend)

Fig. 12: Seismic noise at RSNY. Five time periods (see legend)

Fig. 13: Seismic noise at RSON. Five time periods (see legend)

Fig. 14: Seismic noise at RSSD. Five time periods (see legend)

Fig. 15: Average seismic noise at the five RSTN stations. Comparisons with Queen Creek, AZ, NORSAR, and Lajitas, Texas.

Fig. 16: S-750 self noise comparison with RSNT (quiet time), Lajitas, Texas and NORSAR.

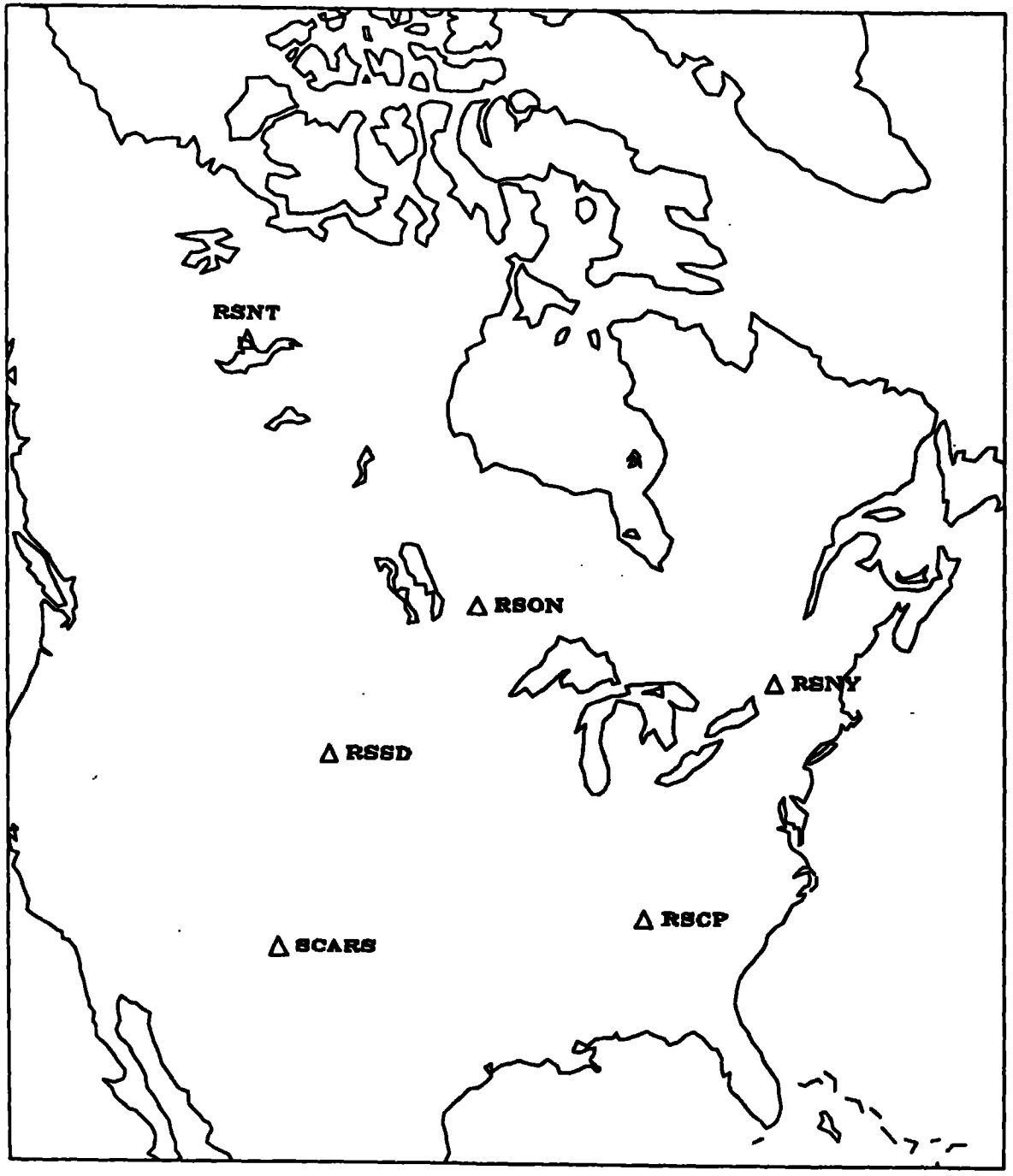
RSNT
RSON
RSNY
RSSD
RSCP
SCARS

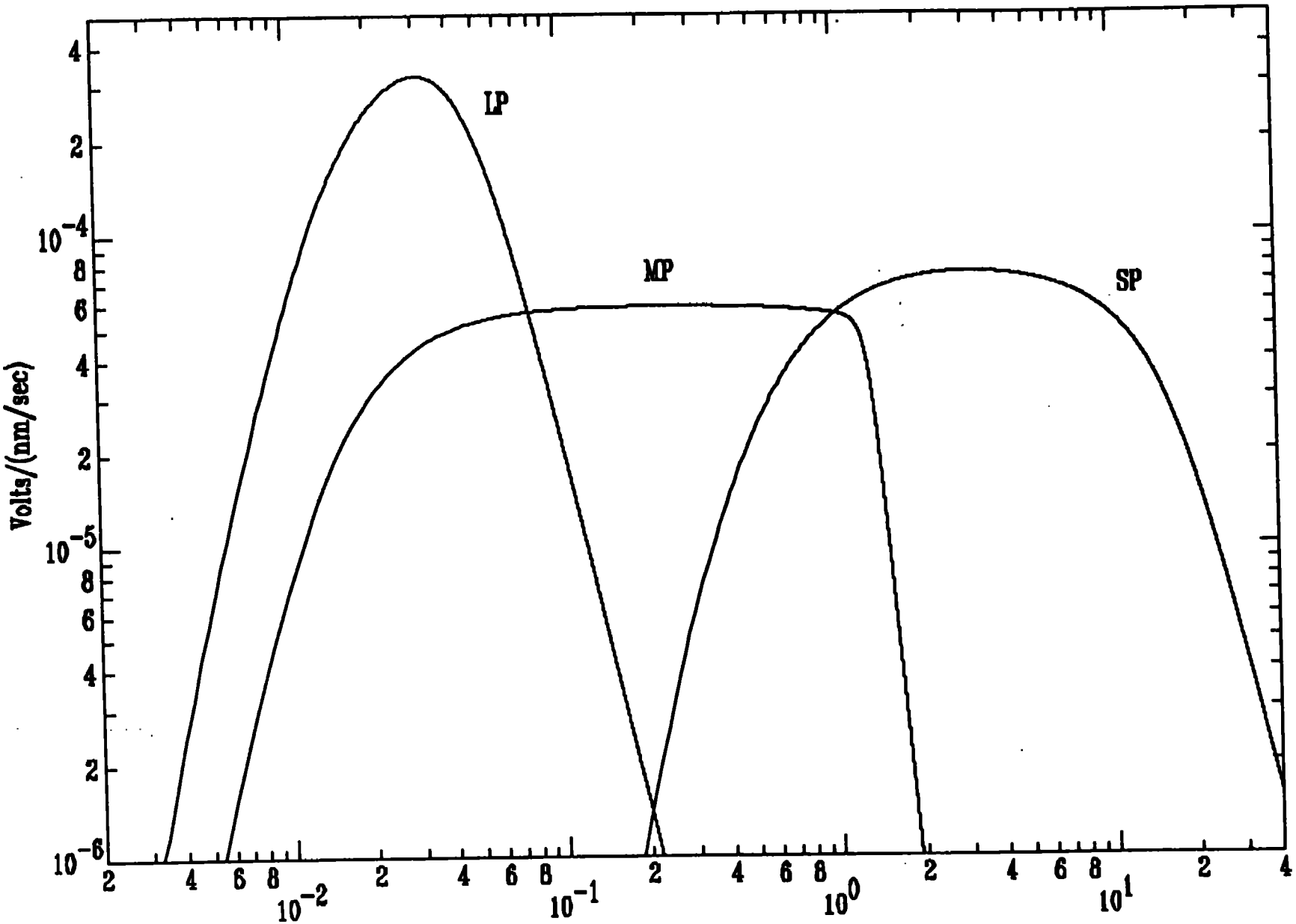
LP
MP
SP
Volts/(nm/sec)
10^{-4}
10^{-5}
10^{-6}
10^{-2}
10^{-1}
10^{0}
10^{1}

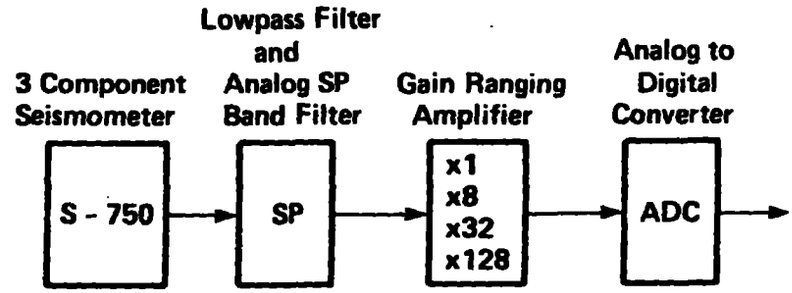
3 Component Seismometer
S - 750
Lowpass Filter and Analog SP Band Filter
SP
Gain Ranging Amplifier
x1
x8
x32
x128
Analog to Digital Converter
ADC

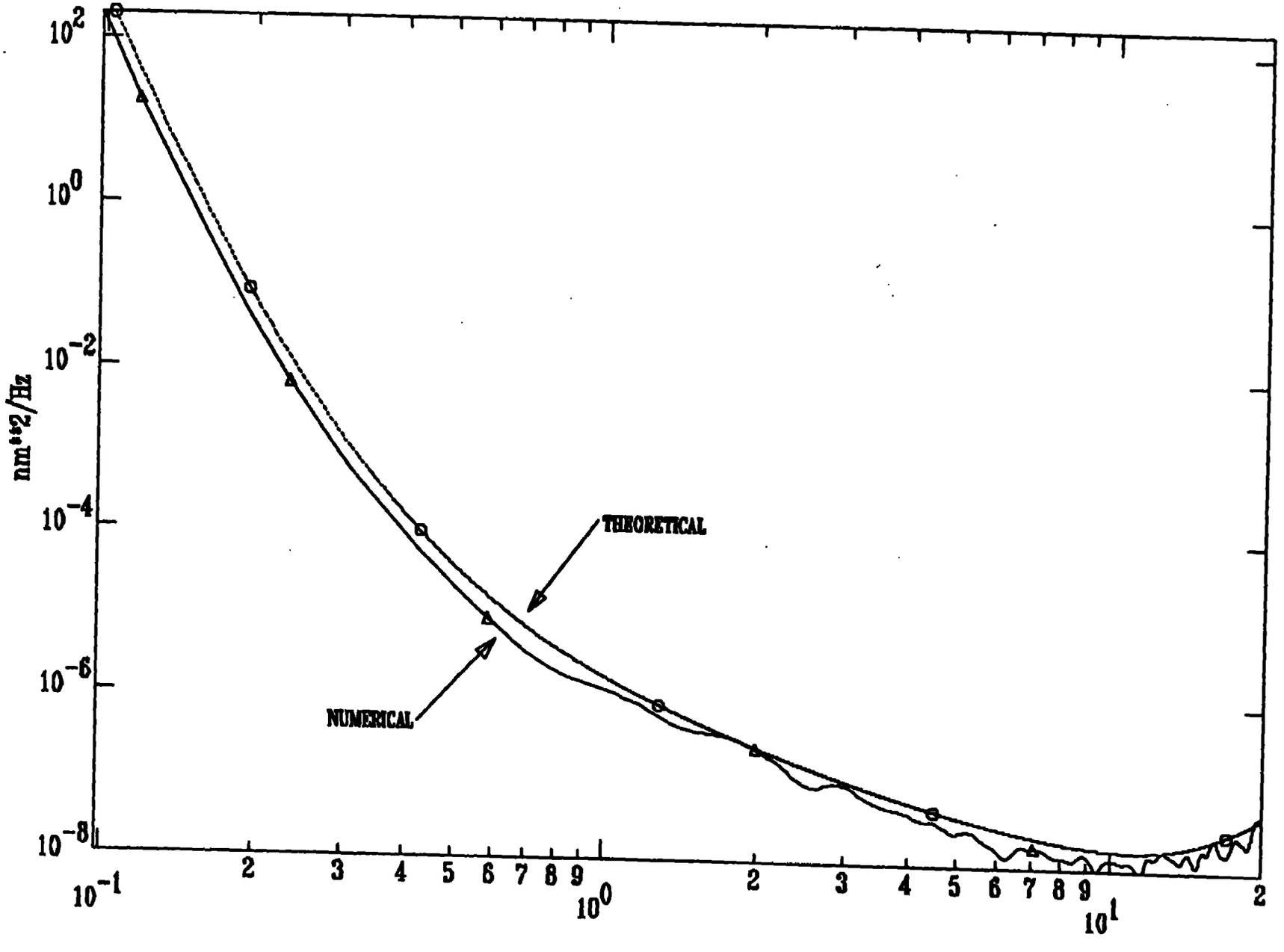
10^2
10^0
10^{-2}
10^{-4}
10^{-6}
10^{-8}
nm**2/Hz
THEORETICAL
NUMERICAL
10^{-1}
2 3 4 5 6 7 8 9
10^0
2 3 4 5 6 7 8 9
10^1
2

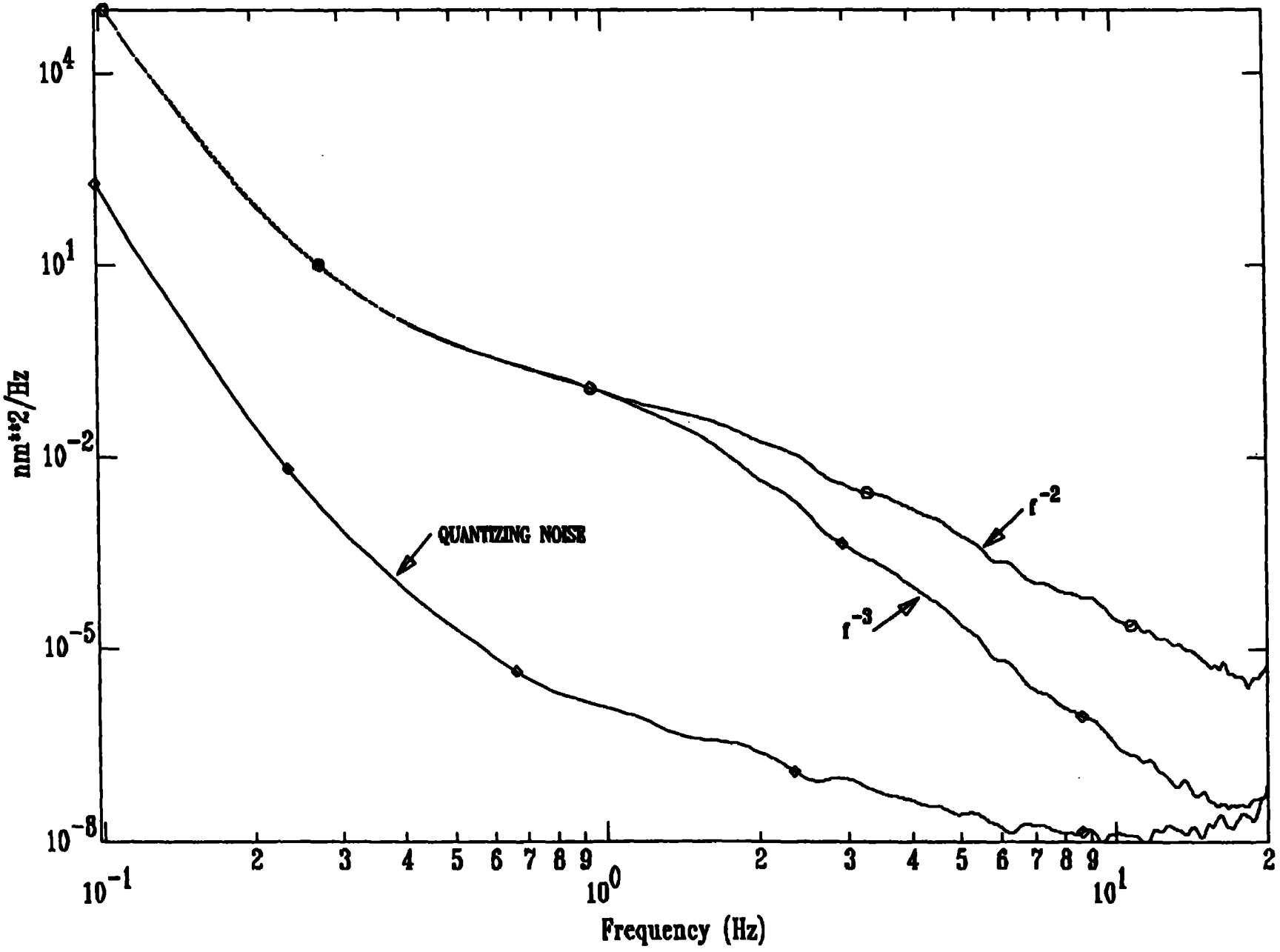
10^4
10^1
10^{-2}
10^{-5}
10^{-8}
nm**2/Hz
QUANTIZING NOISE
f^{-2}
f^{-3}
10^{-1}
10^0
10^1
2 3 4 5 6 7 8 9
Frequency (Hz)

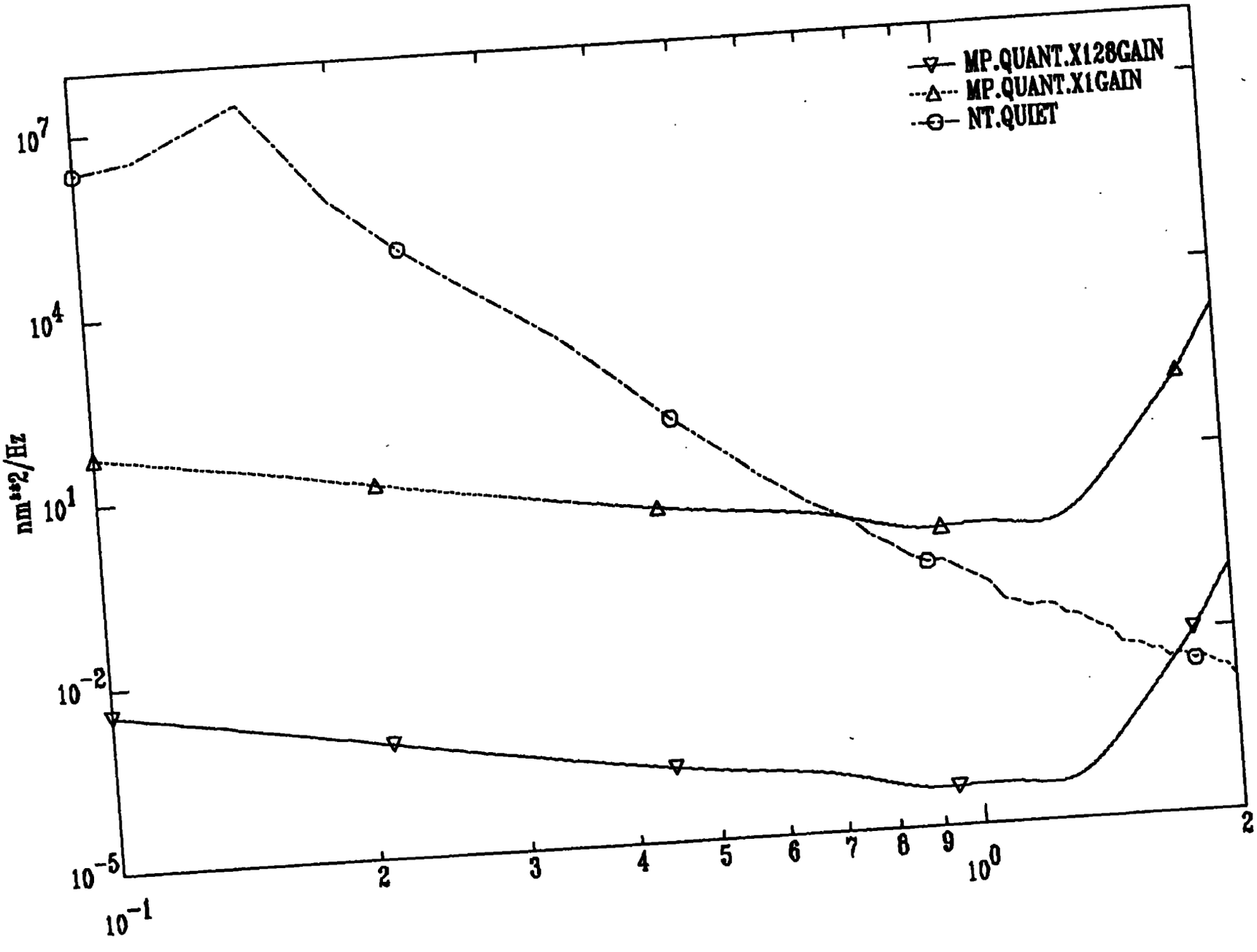
MP.QUANT.X128GAIN
MP.QUANT.X1GAIN
NT.QUIET
10^7
10^4
10^1
10^{-2}
10^{-5}
nm**2/Hz
10^{-1}
2
3
4
5
6
7
8
9
10^0
2

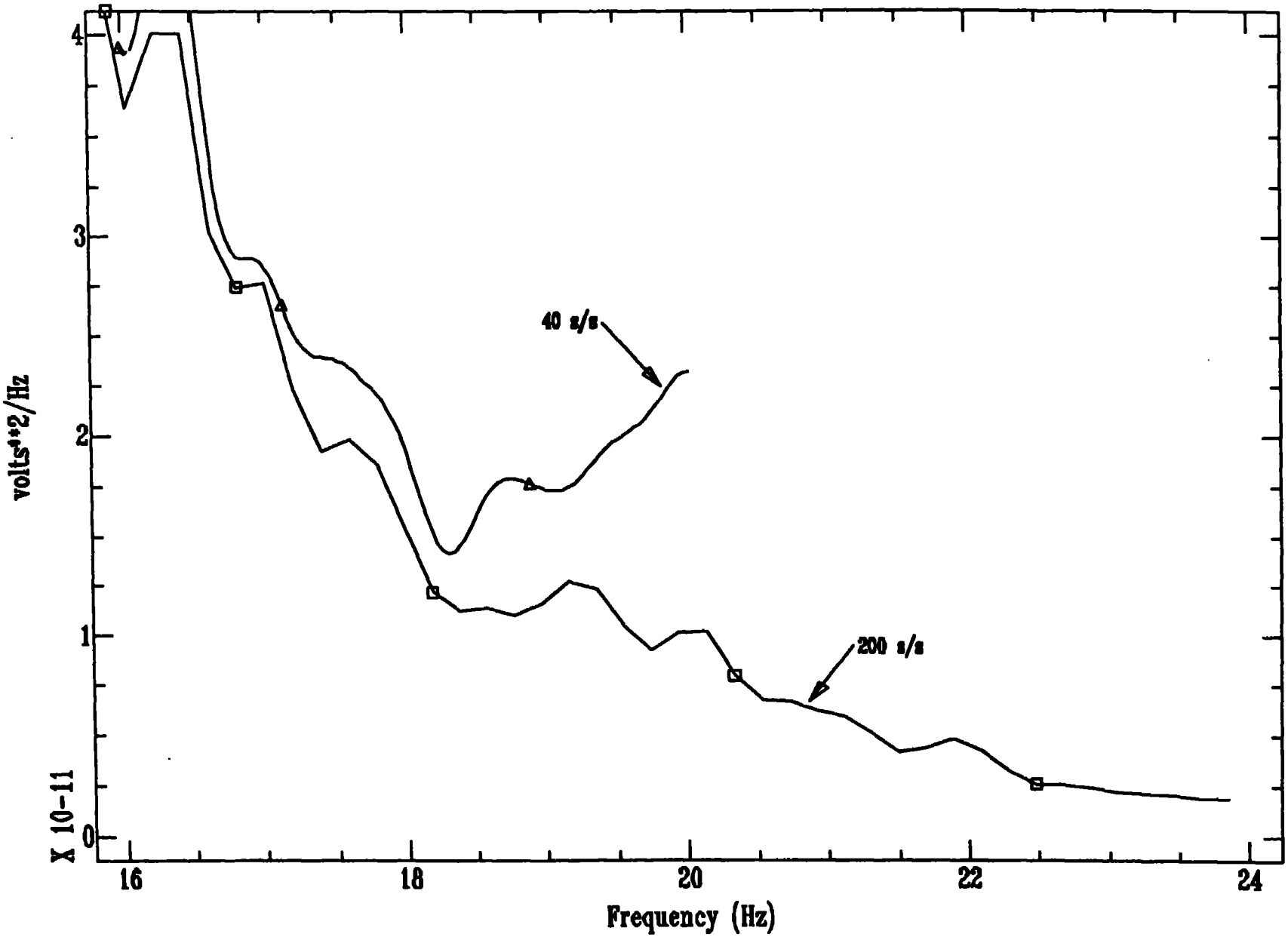
volts**2/Hz
X 10-11
4
3
2
1
0
16
18
20
22
24
Frequency (Hz)
40 s/s
200 s/s

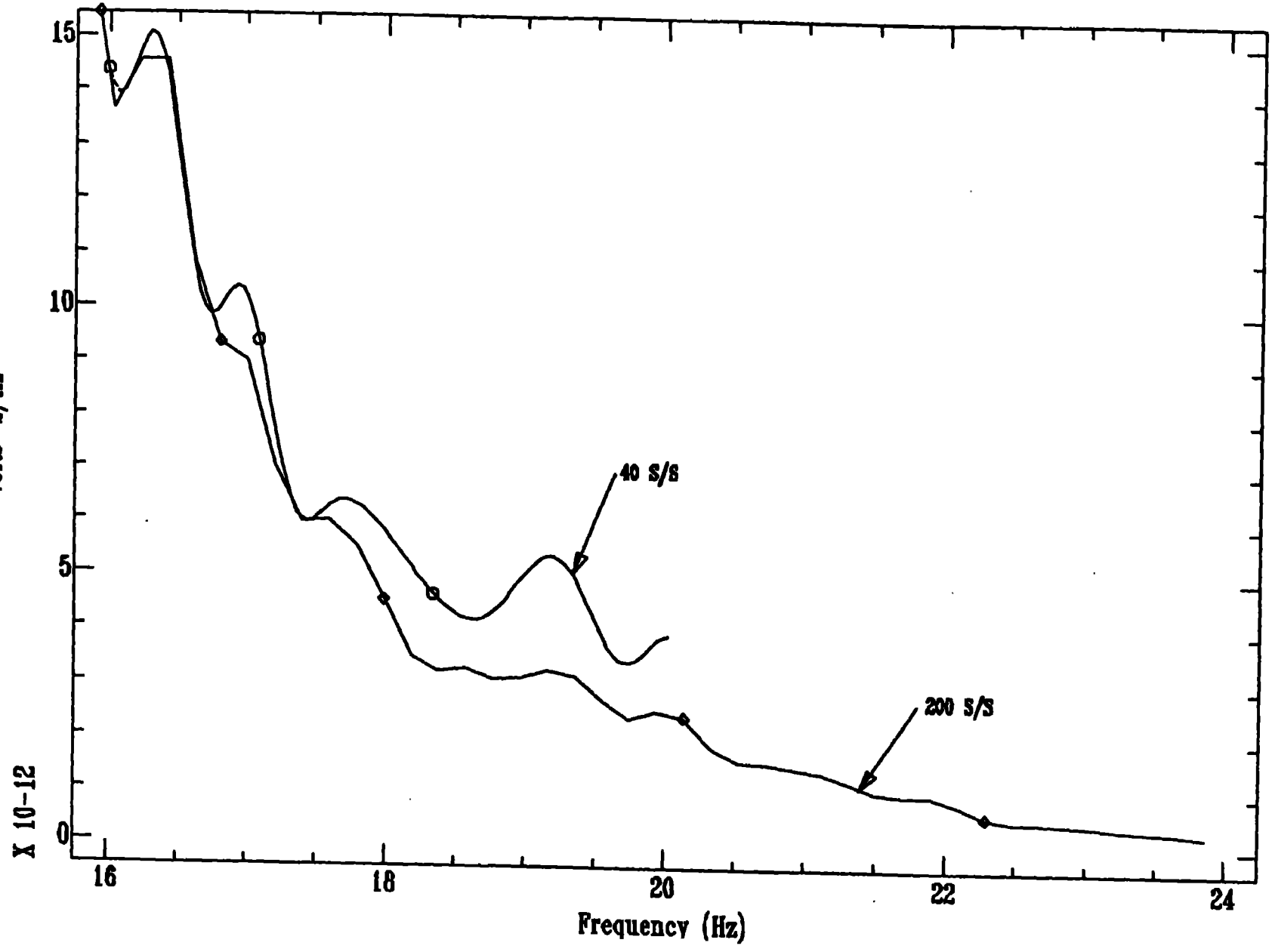
15
10
5
0
X 10-12
volts**2/Hz
40 S/S
200 S/S
16
18
20
22
24
Frequency (Hz)

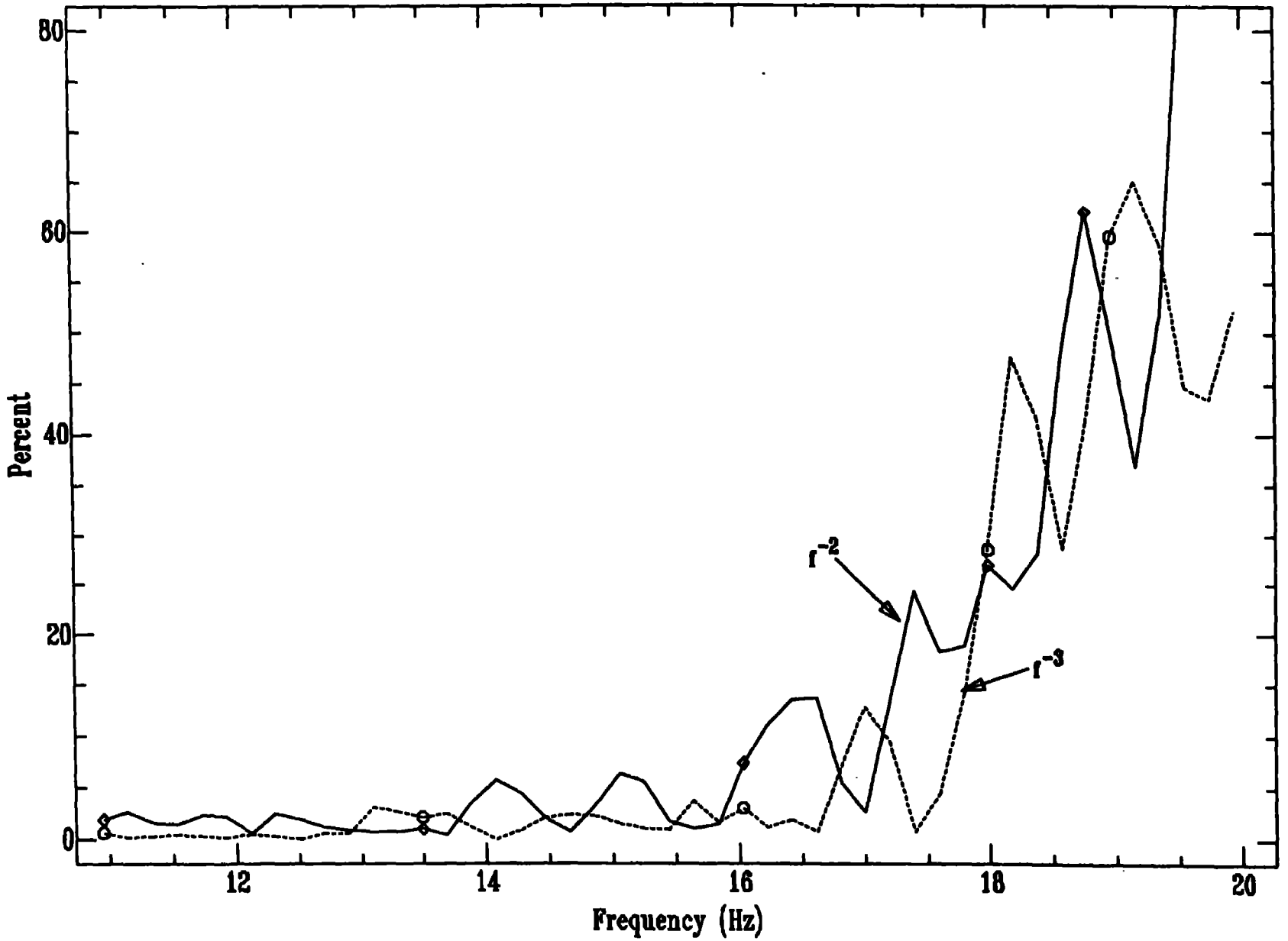
80
60
40
20
0
Percent
12
14
16
18
20
Frequency (Hz)
r^-2
r^-3

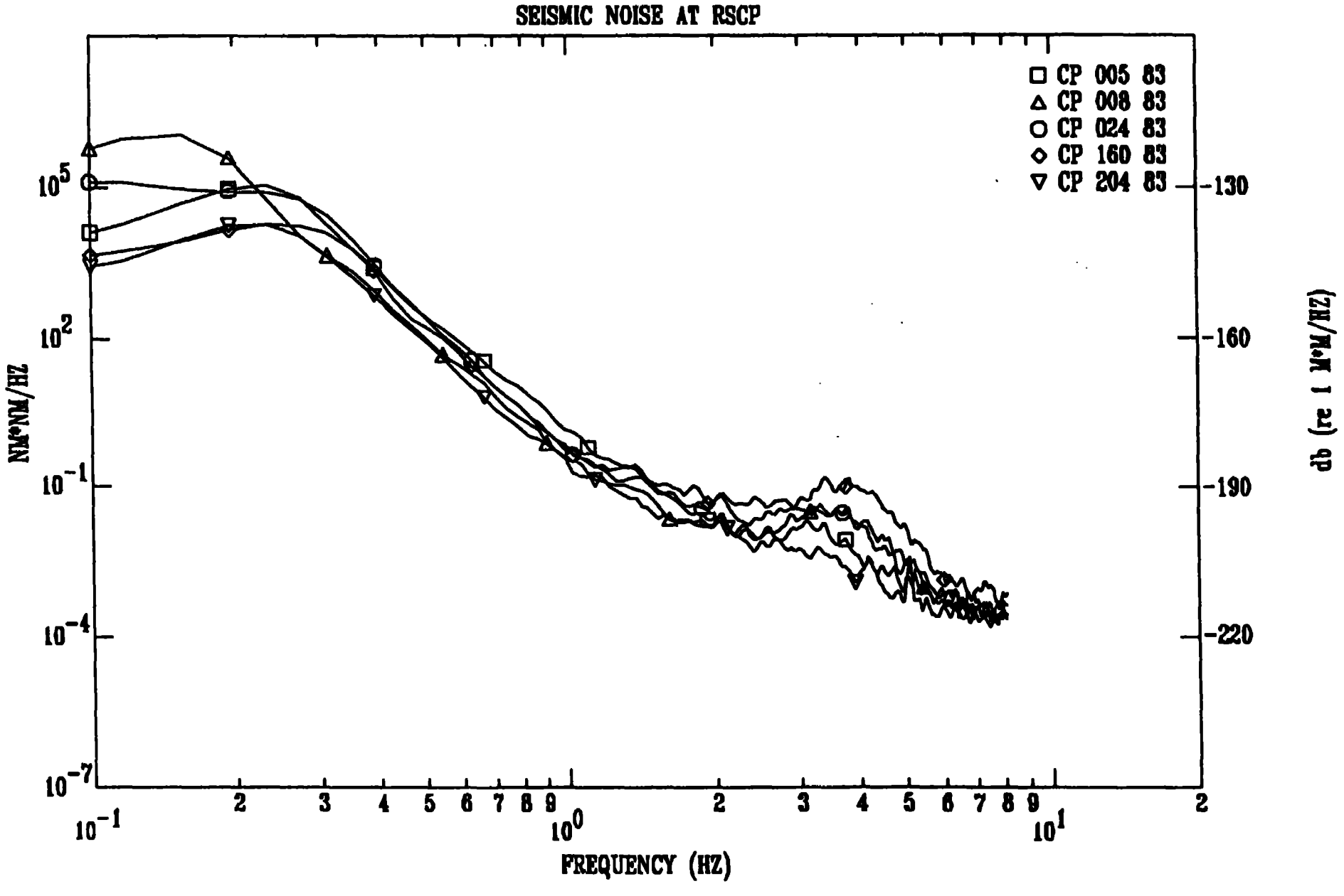
SEISMIC NOISE AT RSCP
CP 005 83
CP 008 83
CP 024 83
CP 160 83
CP 204 83
NM*NM/HZ
db (re 1 M*M/HZ)
FREQUENCY (HZ)
10^5
10^2
10^-1
10^-4
10^-7
10^-1
10^0
10^1
-130
-160
-190
-220

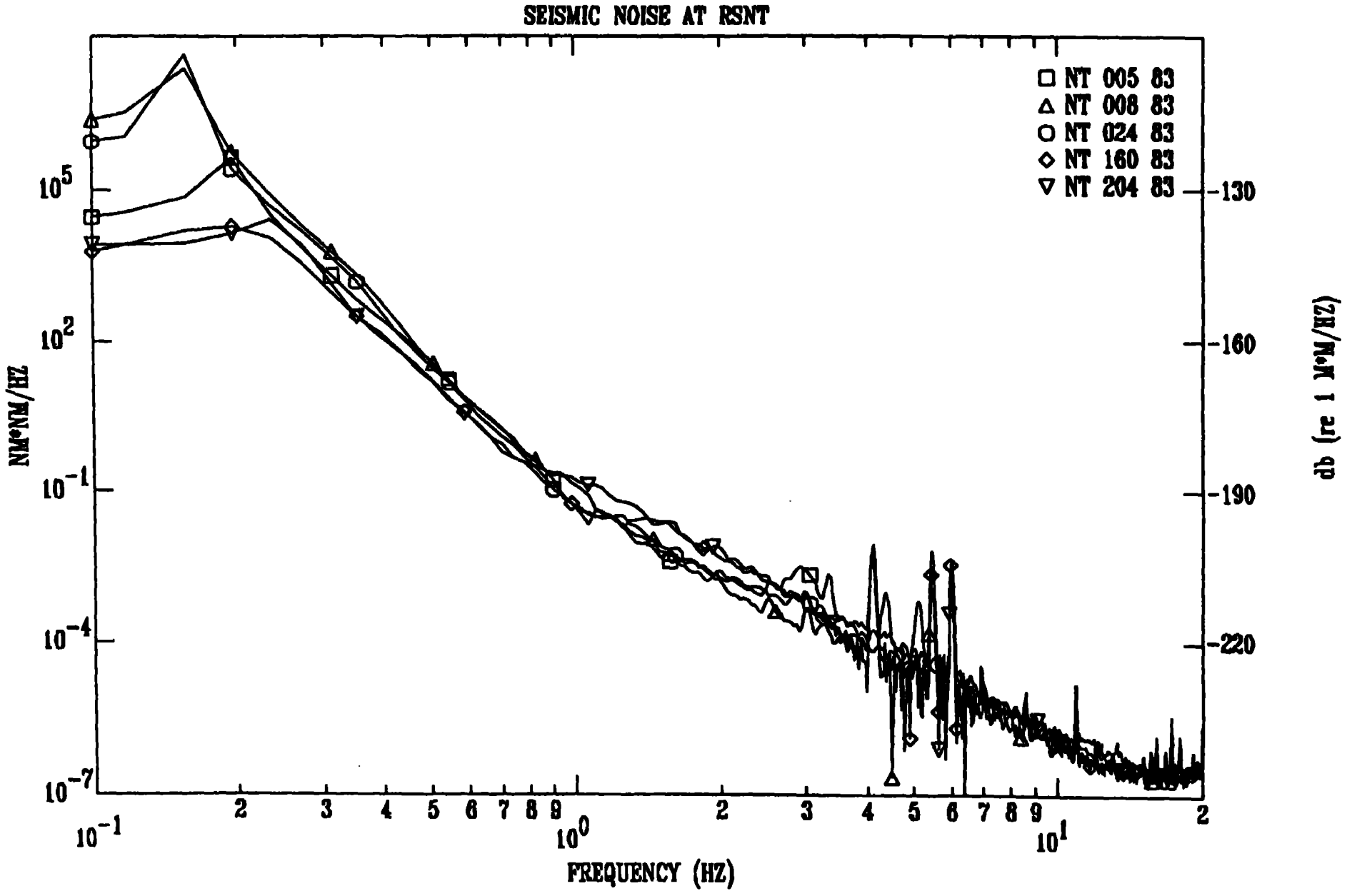
SEISMIC NOISE AT RSNT
NT 005 83
NT 008 83
NT 024 83
NT 160 83
NT 204 83
NM*NM/HZ
db (re 1 M*M/HZ)
FREQUENCY (HZ)
10^5
10^2
10^{-1}
10^{-4}
10^{-7}
-130
-160
-190
-220
10^{-1}
10^0
10^1
2 3 4 5 6 7 8 9

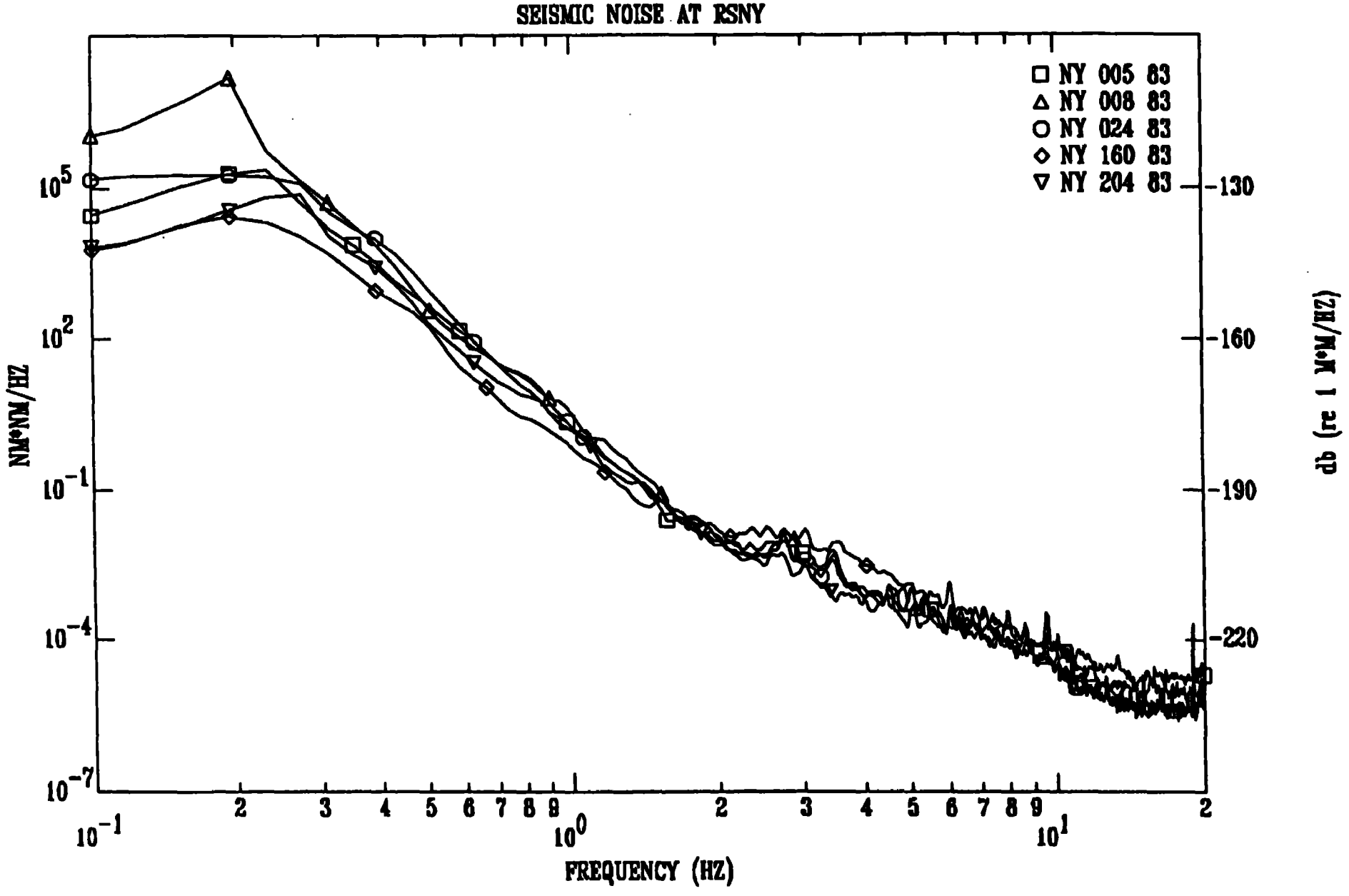
SEISMIC NOISE AT RSNY
NY 005 83
NY 008 83
NY 024 83
NY 160 83
NY 204 83
NM*NM/HZ
db (re 1 M*M/HZ)
FREQUENCY (HZ)
10^5
10^2
10^{-1}
10^{-4}
10^{-7}
-130
-160
-190
-220
10^{-1}
10^0
10^1
2 3 4 5 6 7 8 9

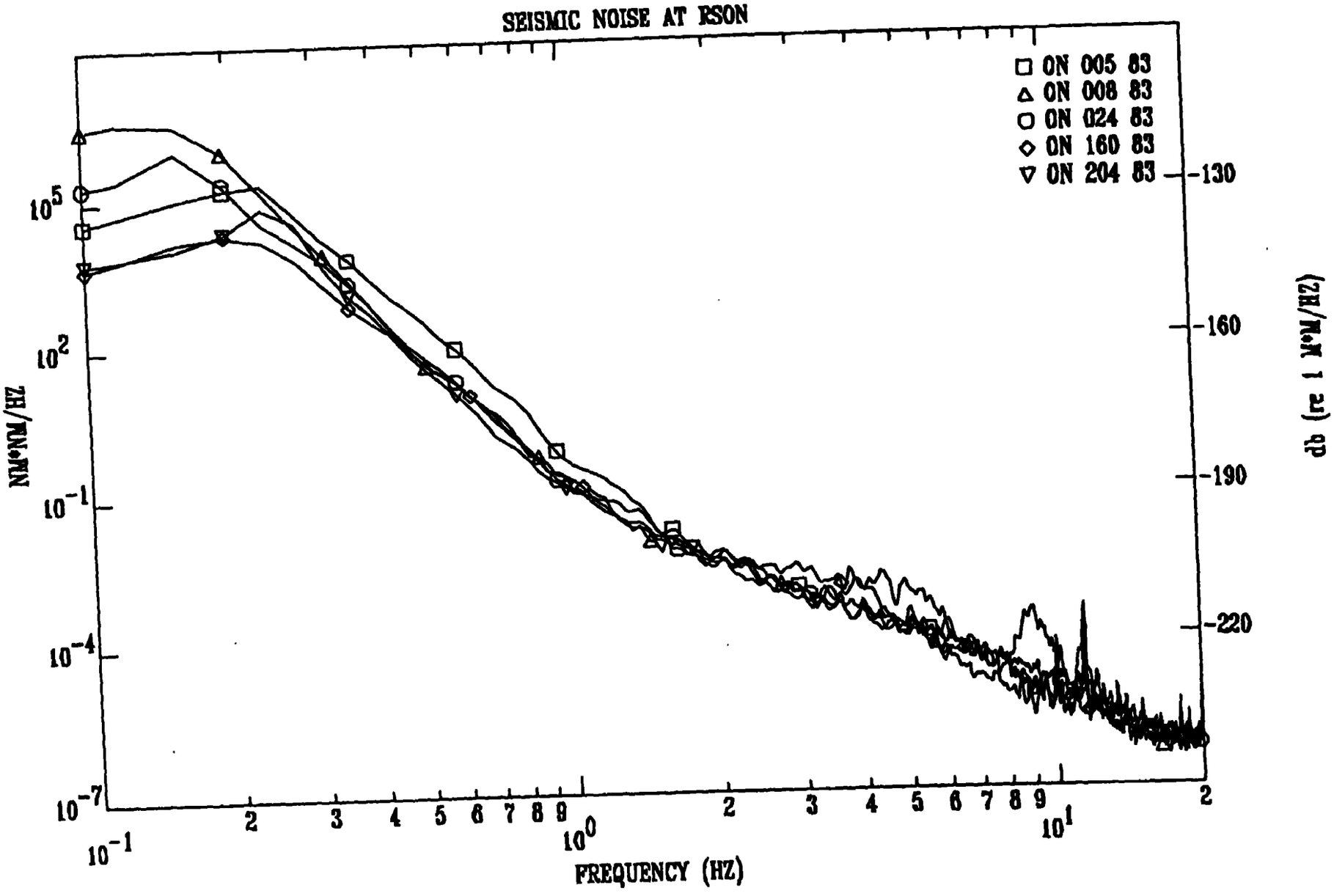
SEISMIC NOISE AT RSON
ON 005 83
ON 008 83
ON 024 83
ON 160 83
ON 204 83
10^5
10^2
10^{-1}
10^{-4}
10^{-7}
NM•NM/HZ
-130
-160
-190
-220
dB (re 1 NM•NM/HZ)
10^{-1}
2 3 4 5 6 7 8 9
10^0
2 3 4 5 6 7 8 9
10^1
2
FREQUENCY (HZ)

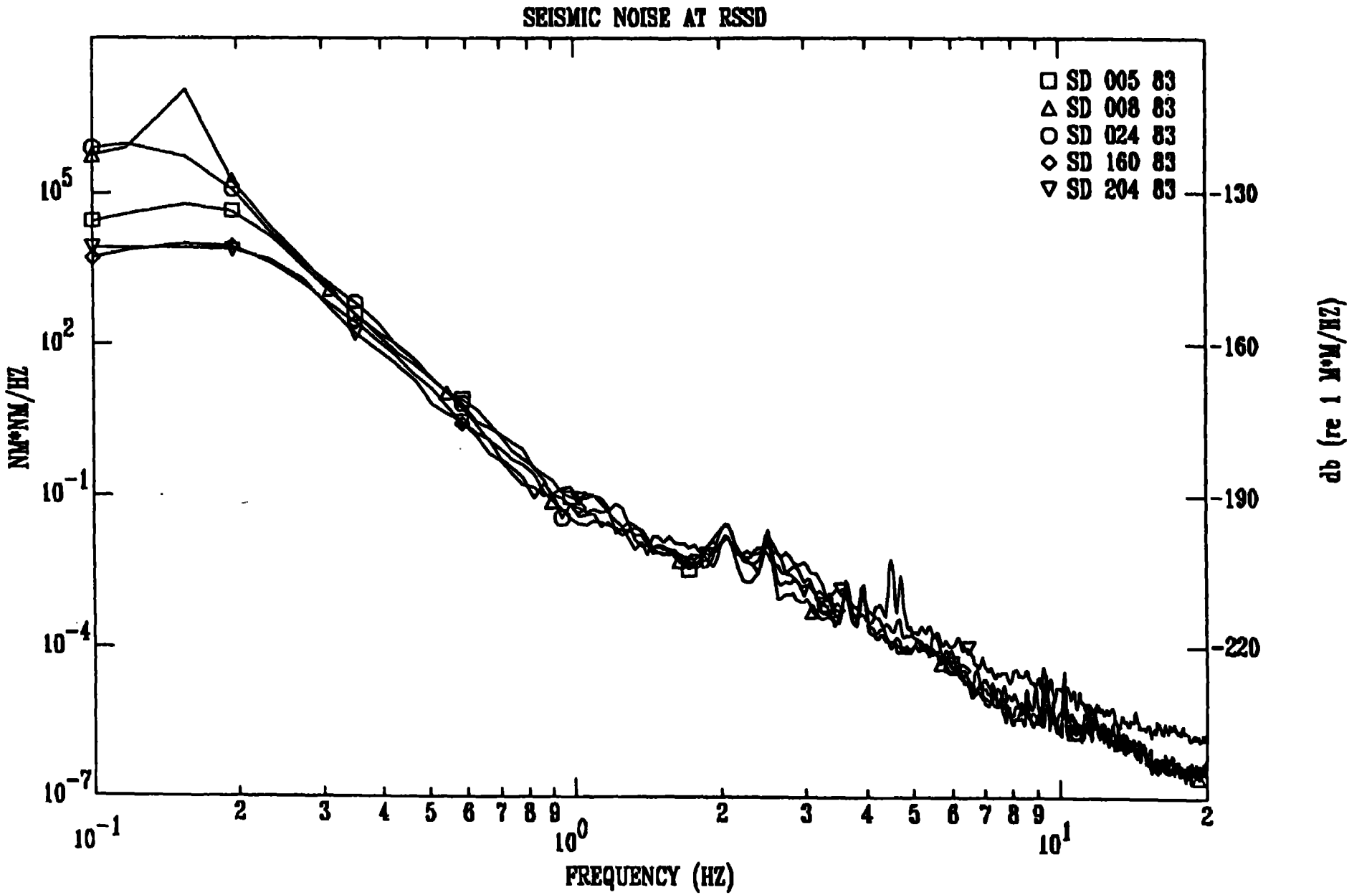
SEISMIC NOISE AT RSSD
SD 005 83
SD 008 83
SD 024 83
SD 160 83
SD 204 83
NM*NM/HZ
db (re 1 M*M/HZ)
FREQUENCY (HZ)
10^{5}
10^{2}
10^{-1}
10^{-4}
10^{-7}
-130
-160
-190
-220
10^{-1}
10^{0}
10^{1}
2
3
4
5
6
7
8
9

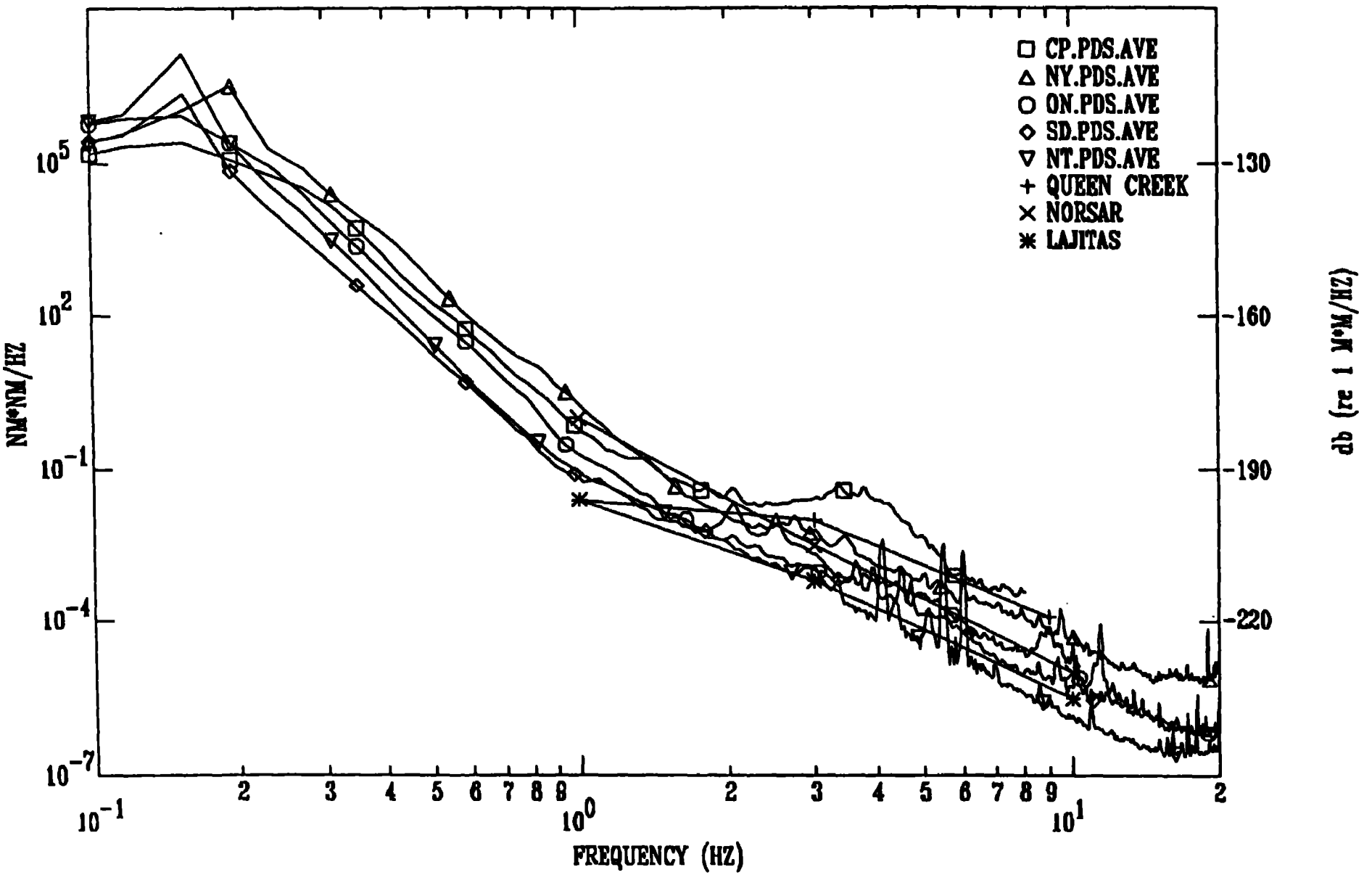
CP.PDS.AVE
NY.PDS.AVE
ON.PDS.AVE
SD.PDS.AVE
NT.PDS.AVE
QUEEN CREEK
NORSAR
LAJITAS
10^5
10^2
10^{-1}
10^{-4}
10^{-7}
-130
-160
-190
-220
10^{-1}
10^0
10^1
2 3 4 5 6 7 8 9
FREQUENCY (HZ)
db (re 1 M*M/HZ)

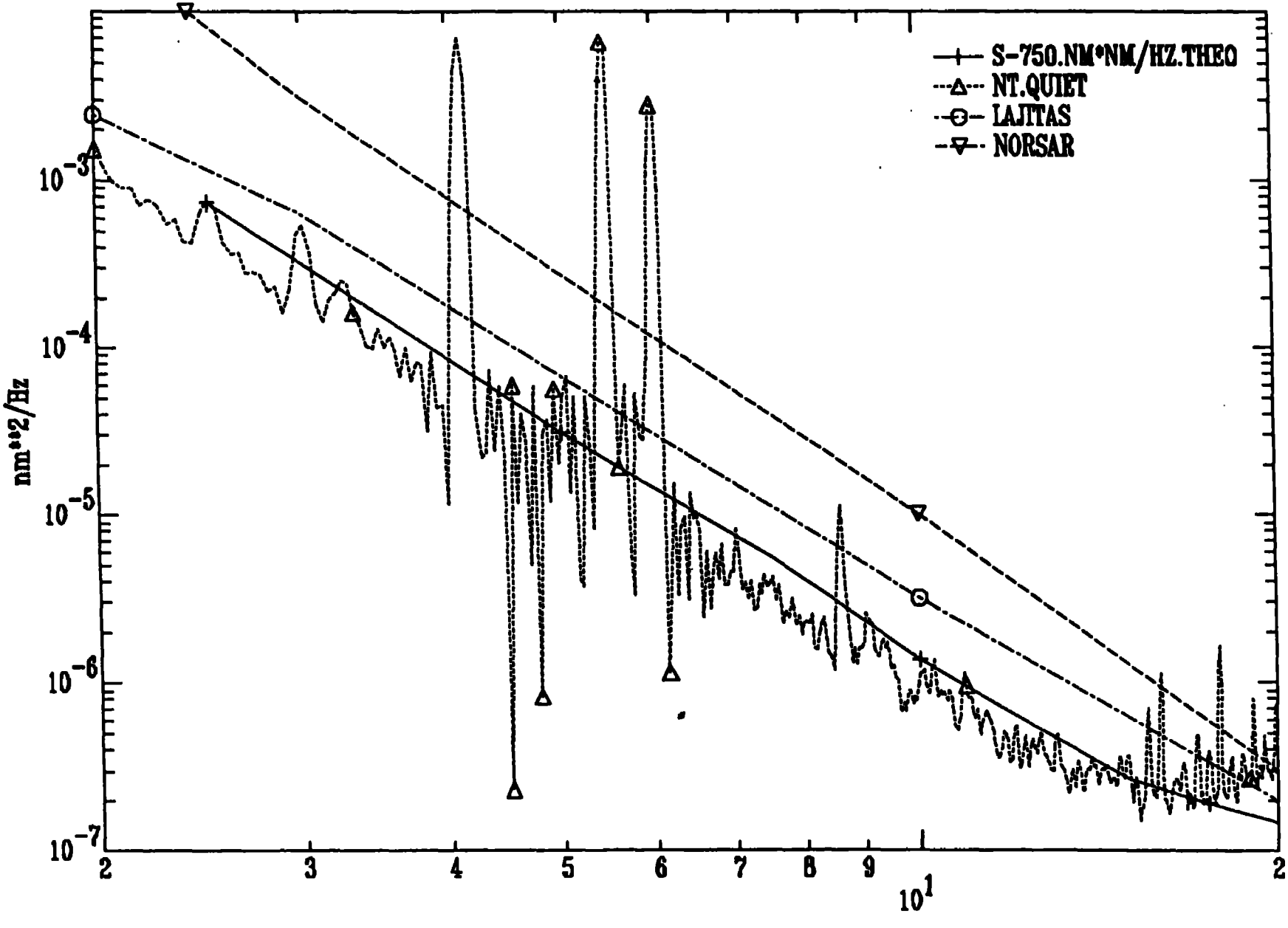
S-750.NM*NM/HZ.THEO
NT.QUIET
LAJITAS
NORSAR
nm**2/Hz
10^{-3}
10^{-4}
10^{-5}
10^{-6}
10^{-7}
2
3
4
5
6
7
8
9
10^{1}
2

REFERENCES

Breding, Dale R. (1983), "Data Users' Guide for the Regional Seismic Test Network (RSTN)," Sandia National Laboratories, Albuquerque, New Mexico 87185

Brune, J. N. and J. Oliver (1959), The Seismic noise of the Earth's Surface, Bull. Seis. Soc. Am., 49, 343-349.

Bungum, H. (1983), Seismic noise at high frequencies, NORSAR Semi-annual Tech. Summary, 1 Oct. 1982 - 31 Mar. 1983.

Durham, H. B. (1984), Personal communications.

Li, T. M. C, J. F. Ferguson, E. Herrin, and H. B. Durham (1984), High-frequency seismic noise at Lajitas, Texas, Bull. Seis. Soc. Am., 74, 2015-2033.

Nuttli, O. W., B. J. Mitchell (1983), "A Methodology for Obtaining Seismic Yield Estimates of Underground Explosions Using Short-Period Lg Waves." Semi-Annual Technical Report No. 1, 1 Oct. 82 - 31 March 1983, ARPA Order 4397, Saint Louis University.

Rodgers, P. W. and C. W. Broadwater (1983), "Comparisons between uphole and downhole seismograms at RSNY and RSSD", UCID-19798. 23 pp.

Rodgers, P. W. and C. W. Broadwater (1984), "Comparisons of uphole and downhole seismograms at RSCP and RSNT", UCID-20087, May 1984.

Starkey, O. D. (1985), Descriptive material regarding the S-750 available from the manufacturer, Teledyne-Geotech. P.O. Box 46 9007, Garland, Texas, 732394.

Stearns, Samuel D. (1975), "Digital Signal Analysis", Sandia Laboratories and the University of New Mexico.

Stokes, P. A. (1982), "The National Seismic Station", Sandia National Laboratory, Albuquerque, NM Sandia Report SAND 81-2134.

Taylor, S. R. (1983), "The Regional Seismic Test Network", Energy and Technology Review, UCRL-52000-83-5, Lawrence Livermore National Laboratory, pp. 20-29.

Taylor, S. R. (1981), "Properties of ambient seismic noise and summary of noise spectrum in the vicinity of RSTN sites," Lawrence Livermore National Laboratory UCID-18928, Jan. 26.

Taylor, S. R. and B. Qualheim (1982): "Regional Seismic Test Network Descriptions," Lawrence Livermore National Laboratory UCID-19769, March.

Taylor, S. R. (1984), "Analysis of the Goodnow, NY earthquake using RSTN data," UCID-20129,. Lawrence Livermore National Laboratory, Livermore, CA 94550.

2485H